PHYSICAL REVIEW D **93,** 075033 (2016)

750 GeV diphoton resonance as a singlet scalar in an extra dimensional model

Chengfeng Cai (蔡成丰),[1] Zhao-Huan Yu (余钊焕),[2] and Hong-Hao Zhang (张宏浩)[1,*]

[1]*School of Physics, Sun Yat-Sen University, Guangzhou 510275, China*

[2]*ARC Centre of Excellence for Particle Physics at the Terascale, School of Physics, The University of Melbourne, Victoria 3010, Australia*

(Received 4 January 2016; published 26 April 2016)

We interpret the 750 GeV diphoton excess recently found in the 13 TeV LHC data as a singlet scalar in an extra dimensional model, where one extra dimension is introduced. In the model, the scalar couples to multiple vectorlike fermions, which are just the Kaluza-Klein modes of SM fermions. Mediated by the loops of these vectorlike fermions, the ϕ effective couplings to gluons and photons can be significantly large. Therefore, it is quite easy to obtain an observed cross section for the diphoton excess. We also calculate the cross sections for other decay channels of ϕ, and find that this interpretation can evade the bounds from the 8 TeV LHC data.

DOI: 10.1103/PhysRevD.93.075033

I. INTRODUCTION

Recently, the ATLAS collaboration reported an excess at ~750 GeV in the diphoton invariant mass distribution, based on the 13 TeV LHC data with an integrated luminosity of 3.2 fb^{-1} [1]. Assuming this excess is due to a resonance, the local (global) signal significance is 3.9σ (2.3σ). A very preliminary fit showed that the resonance has a broad width of ~45 GeV. However, since the statistics of the current data is not quite sufficient, the measurement of the width should be treated as a hint rather than a final conclusion. On the other hand, a similar excess at ~760 GeV have also been found by the CMS collaboration based on a data set of 2.6 fb^{-1}, but the local (global) significance is lower and just 2.6σ (1.2σ) [2].

These exciting results have stimulated lots of theoretical interpretations [3–99]. Although some works suggested this excess may be due to a spin-2 particle [49,50] or a spin-1 particle[1] [47,70,92,102], most of these works interpreted it as a new scalar (ϕ) beyond the standard model (SM). New scalars can be naturally introduced from the Higgs sector in many SM extensions. However, since the observed cross section for $pp \to \phi \to \gamma\gamma$ is $\sim\mathcal{O}(10)$ fb, ordinary two-Higgs-doublet and supersymmetric models could not give such a large production cross section without further extensions [6,9,12].

As LHC is a pp collider, parton distribution functions determine that gg fusion happens much more often than $q\bar{q}$ annihilation. Besides, ϕ couplings to quarks are usually proportional to quark masses in many models. Therefore, gg fusion should be the dominant process for $pp \to \phi$ production. In order to increase the $pp \to \phi \to \gamma\gamma$ production rate, the ϕ couplings to gg and $\gamma\gamma$, which are generally induced by loop processes, need to be significantly enhanced. This can be achieved by introducing multiple electrically charged and colored vectorlike fermions coupled to ϕ [6,20,42,73,87,93]. The vectorlike feature is particularly appealing for avoiding gauge anomalies.

It is well known that it is possible to extend the SM with TeV-scale extra dimensions [103], which may induce remarkable signals at the LHC. In this work, we give a reasonable origin for such vectorlike fermions: they are Kaluza-Klein (KK) modes of SM fermions in an SM extension where just one compactified extra dimension is introduced. We assume that there is a 5D CP-even singlet scalar field Φ that couples to all 5D fermion fields and generates their bulk mass terms by obtaining a nonzero vacuum expectation value (VEV). Once nonzero bulk masses are generated, the profiles of the zero modes will be exponential functions so that the zero modes are localized at either end of the interval of the fifth dimension. The localization of fermions is especially attractive because it can give an explanation to the fermion mass hierarchy problem [104–108]. Consequently, although the 5D fermions are born as vectorlike fields, their zero modes will be chiral after imposing Dirichlet boundary conditions and become the usual SM fermions, while higher KK modes remain vectorlike.

Here this localizing feature is caused by the scalar VEV, thus Φ is called the localizer [105]. We assume the excitation around the VEV of the zero mode of Φ is the observed 750 GeV scalar ϕ. ϕ automatically couples to the KK modes of the fermions, which are vectorlike and charged under the electroweak gauge symmetry. Therefore ϕ can be produced through the gluon-gluon fusion process induced by the KK quark loops and then decays into

*zhh98@mail.sysu.edu.cn

[1]In this case, the decay products of the resonance should involve, besides two photons, at least one extra particle. Otherwise it would contradict the Landau-Yang theorem [100,101].

two photons induced by the KK quark and KK charged lepton loops.

Rather than covering complicated setups, we fully simplify the model and just focus on how to explain the diphoton excess. Therefore, the gluon-gluon fusion process is assumed to be the only source for $pp \to \phi$ production. After production, ϕ decays into gg, $\gamma\gamma$, ZZ, γZ, and W^+W^- through loops, as well as hh at the tree level, which would be suppressed if the mixing between ϕ and the SM Higgs is small. We will calculate the cross sections for these processes and demonstrate that the model is consistent with all existed bounds.

The paper is organized as follows. In Sec. II we briefly introduce the model. In Sec. III we discuss the KK modes of ϕ and the mixing between ϕ and the Higgs. Section IV presents our interpretation to the 750 GeV diphoton excess and shows that it is consistent with 8 TeV LHC bounds. Section V gives the conclusion. In Appendix A, we list the relevant interaction Lagrangians involved in our calculation. Appendix B gives a supplementary discussion on the case that the Yukawa couplings of the singlet fermions have the same signs as the doublet fermions.

II. THE MODEL

We discuss a quite simplified model, which is similar to the one in Ref. [105]. We assume all fields corresponding to SM particles are living in a flat 5D space-time. Rather than considering a orbifold structure and orbifold boundary conditions [109], we simply adopt a compactified interval as the fifth dimension. The usual 4D coordinates and the extra dimensional coordinate are denoted as x^μ and $y \in [0, \pi R]$, respectively. As in universal extra dimensions [110], we assume that the usual four-dimensional components of gauge field zero modes have flat profiles $f_{\text{gauge}}(y) = 1/\sqrt{\pi R}$ while their fifth components vanish. This can be obtained by imposing a Dirichlet boundary condition on the fifth component $A_y = 0$ at $y = 0$ and πR, and a Neumann boundary condition on the four-dimensional components $\partial_y A_\mu = 0$ at $y = 0$ and πR.

The Higgs doublet field distributes in the 5D spacetime with a flat VEV, and its zero mode also has a flat profile. Apart from the Higgs, a new 5D singlet scalar Φ is introduced. We assume the VEV of Φ is flat, in order to generate constant bulk masses for all fermions. The 5D Higgs H and the new singlet scalar Φ are assumed to satisfy the Neumann boundary conditions at both ends of the fifth interval, and their mode decompositions will be given in detail in Sec. III [see Eqs. (25) and (26)].

After solving the equation of motion with proper boundary conditions on the fermions, we can obtain chiral zero-mode fermions, which play the role of ordinary SM fermions. The profiles of these zero modes are localized at either end of the interval and exponentially spread into the fifth dimension.

To be concrete, let us consider the action describing a 4-component 5D fermion Ψ coupled to Φ as

$$\begin{aligned} S &= \int d^5x \overline{\Psi}(i\Gamma^M D_M - \tilde{y}_f \Phi)\Psi \\ &= \int d^5x \overline{\Psi}(i\Gamma^M D_M - \tilde{y}_f \langle\Phi\rangle - \tilde{y}_f \tilde{\Phi})\Psi, \end{aligned} \tag{1}$$

where Γ^M is the gamma matrices with the fifth matrix defined as $\Gamma^5 = i\gamma^5$. The covariant operator $D_M = \partial_M - i\tilde{g}A_M$, where A_M is a gauge field and $\tilde{g}$ is a gauge coupling with a mass dimension of $-1/2$. After Φ develops a VEV v_ϕ, the fermion acquires a bulk mass

$$M_f = \tilde{y}_f \langle\Phi\rangle = y_f v_\phi, \tag{2}$$

where $y_f = \tilde{y}_f/\sqrt{\pi R}$ is a dimensionless Yukawa coupling. $\tilde{\Phi}$ is the excitation around the VEV. Note that in principle one can also include a generic bulk mass term $M_\Psi \overline{\Psi}\Psi$, and then the total bulk mass would be no longer proportional to the Yukawa coupling. As this term introduces one more parameter, the interpretation to the diphoton excess would be easier. For simplicity and as the first step of the probe, below we neglect this term and show that the model can well explain the excess even without it.

The kinetic and bulk mass terms in the action (1) give the following equation of motion for a free fermion field:

$$\begin{pmatrix} \partial_y - M_f & i\sigma^\mu \partial_\mu \\ i\bar{\sigma}^\mu \partial_\mu & -\partial_y - M_f \end{pmatrix} \begin{pmatrix} \Psi_L \\ \Psi_R \end{pmatrix} = 0. \tag{3}$$

Dirichlet boundary conditions will be imposed on either the left-handed or the right-handed component of Ψ. These two components can be decomposed in modes:

$$\Psi_L = \sum_{n=0}^{\infty} \chi_a^{(n)}(x) f^{(n)}(y), \qquad \Psi_R = \sum_{n=0}^{\infty} \xi^{(n)\dagger \dot{a}}(x) g^{(n)}(y). \tag{4}$$

Substituting the mode decomposition into Eq. (3), we obtain

$$\begin{aligned} (-\partial_y + M_f) f^{(n)}(y) &= m_n g^{(n)}(y), \\ (\partial_y + M_f) g^{(n)}(y) &= m_n f^{(n)}(y). \end{aligned} \tag{5}$$

Thus the 4D field of each mode satisfies the Dirac equation.

The profile of a zero mode with a zero mass ($m_0 = 0$) is $f^{(0)}(y) \propto e^{M_f y}$ and $g^{(0)}(y) \propto e^{-M_f y}$. Then if we impose the Dirichlet boundary condition that $\Psi_R = 0$ ($\Psi_L = 0$) at $y = 0$ and πR, we will have $g^{(0)}(y) = 0$ ($f^{(0)}(y) = 0$), which means that the zero mode is chiral as desired for SM fermions. Note that the zero mode here does not have mass,

which can be acquired from the ordinary Higgs mechanism as we will see below.

On the other hand, the KK modes ($n \geq 1$) are vectorlike, i.e., their left-handed and right-handed components transform as the same under a gauge symmetry. The profiles of these KK modes can be exactly solved. If the boundary condition is $\Psi_R = 0$ at $y = 0$ and πR, then

$$f^{(n)}(y) = \sqrt{\frac{2/(\pi R)}{M_f^2 + n^2/R^2}}\left(\frac{n}{R}\cos\frac{ny}{R} + M_f \sin\frac{ny}{R}\right), \tag{6}$$

$$g^{(n)}(y) = \sqrt{\frac{2}{\pi R}}\sin\frac{ny}{R}. \tag{7}$$

The mass of the n-mode is given by $m_n^2 = M_f^2 + n^2 M_{\rm KK}^2$ ($n \geq 1$), where $M_{\rm KK} \equiv R^{-1}$. These profiles satisfy the orthogonality conditions

$$\int_0^{\pi R} dy f^{(m)}(y) f^{(n)}(y) = \delta_{mn},$$
$$\int_0^{\pi R} dy g^{(m)}(y) g^{(n)}(y) = \delta_{mn}. \tag{8}$$

In this model, we assume that the 5D fermion fields for $SU(2)_L$ doublet fermions have this kind of boundary conditions, so that their zero modes are left-handed. For the 5D fermion fields for $SU(2)_L$ singlet fermions, we impose the boundary condition that $\Psi_L = 0$ at $y = 0$ and πR, and hence their zero modes are right-handed.

Substituting the mode expansion of Ψ into the action, we can obtain the couplings between $\tilde{\Phi}$ and each mode of the fermion. After integrating out the fifth dimension coordinate, the effective 4D action of the Yukawa interactions corresponding to a fermion with a left-handed zero mode can be expressed as

$$\begin{aligned} S_{\phi\overline{F}F} = \int d^4x \Bigg\{ & -y_f \sum_{n=1}^{\infty} \frac{M_f}{\sqrt{M_f^2 + n^2 M_{\rm KK}^2}} \phi(x) \overline{F}^{(n)}(x) F^{(n)}(x) \\ & - \frac{2y_f}{\sqrt{\pi}} \sqrt{\frac{M_f}{e^{2\pi M_f/M_{\rm KK}} - 1}} \sum_{n=1}^{\infty} \frac{n M_{\rm KK}^{3/2} [1 - \cos(n\pi) e^{\pi M_f/M_{\rm KK}}]}{M_f^2 + n^2 M_{\rm KK}^2} \phi(x) [\overline{F}^{(n)}(x) F_L^{(0)}(x) + \text{H.c.}] \\ & - \frac{y_f}{\pi} \sum_{m \pm n = \text{odd}} \frac{4mn}{n^2 - m^2} \frac{M_{\rm KK}}{\sqrt{M_f^2 + m^2 M_{\rm KK}^2}} \phi(x) [\overline{F}^{(n)}(x) F_L^{(m)}(x) + \text{H.c.}] \Bigg\}, \end{aligned} \tag{9}$$

where the 4D scalar field $\phi(x)$ corresponds to the zero mode of $\tilde{\Phi}$, and $F^{(n)}(x)$ is the 4D n-mode Dirac fermion. For $n \geq 1$, $F^{(n)}(x)$ is vectorlike. Note that there is no $\phi\overline{F}^{(0)}F^{(0)}$ coupling in the action (9). With respect to the fermion content of the SM, we should introduce three generations of quark doublets Q, quark singlets U and D, lepton doublets L, and lepton singlets E and N. The interactions between the doublet fields and ϕ are just given by Eq. (9) with F substituted by Q and L. The interactions between the singlet fields and ϕ will be discussed in next paragraph [see Eq. (12)]. The coupling in the first line of Eq. (9) will contribute to the LHC production and decay of ϕ through loop processes. If the bulk mass M_f vanishes, the $\phi\overline{F}^{(n)}F^{(n)}$ couplings would vanish as well, even in the case that y_f is nonzero and M_f is tuned to be zero by adding another constant bulk mass to compensate $\tilde{y}_f\langle\Phi\rangle$. Therefore, a nonzero bulk mass is necessary for loop production and decay of ϕ in this model.

For simplicity, we assume that $\tilde{y}_q$ and $\tilde{y}_l$ are universal for all quarks and leptons, respectively. For the $SU(2)_L$ fermions, we assume that the singlet Yukawa couplings to Φ are opposite to the corresponding doublet Yukawa couplings. That is to say, the Yukawa terms for the quark doublet Q and the lepton doublet L can be given by $-\tilde{y}_q\Phi\overline{Q}Q - \tilde{y}_l\Phi\overline{L}L$, while those for the singlets U, D, and E are $+\tilde{y}_q\Phi\overline{U}U + \tilde{y}_q\Phi\overline{D}D + \tilde{y}_l\Phi\overline{E}E$. Then the profiles of the KK modes of a doublet has the forms of Eqs. (6) and (7), while the profiles of the KK modes of a singlet are given by

$$f_s^{(n)}(y) = -\sqrt{\frac{2}{\pi R}}\sin\frac{ny}{R}, \tag{10}$$

$$g_s^{(n)}(y) = \sqrt{\frac{2/\pi R}{M_f^2 + n^2/R^2}}\left(\frac{n}{R}\cos\frac{ny}{R} + M_f \sin\frac{ny}{R}\right). \tag{11}$$

The corresponding interactions with ϕ are

$$S_{\phi\overline{F}'F'} = \int d^4x \Big\{ -y_f \sum_{n=1}^{\infty} \frac{M_f}{\sqrt{M_f^2 + n^2 M_{\rm KK}^2}} \phi(x) \overline{F}'^{(n)}(x) F'^{(n)}(x) - \frac{2y_f}{\sqrt{\pi}} \sqrt{\frac{M_f}{e^{2\pi M_f/M_{\rm KK}} - 1}} \sum_{n=1}^{\infty} \frac{n M_{\rm KK}^{3/2} [1 - \cos(n\pi) e^{\pi M_f/M_{\rm KK}}]}{M_f^2 + n^2 M_{\rm KK}^2} \phi(x) [\overline{F}'^{(n)}(x) F_R'^{(0)}(x) + \text{H.c.}] - \frac{y_f}{\pi} \sum_{m \pm n = \text{odd}} \frac{4mn}{n^2 - m^2} \frac{M_{\rm KK}}{\sqrt{M_f^2 + m^2 M_{\rm KK}^2}} \phi(x) [\overline{F}'^{(n)}(x) F_R'^{(m)}(x) + \text{H.c.}] \Big\}, \tag{12}$$

where $F' = U, D, E, N$. Note that the first lines of Eqs. (9) and (12) have the same form. By making the signs of the Yukawa couplings to be opposite, $g_s^{(n)}(y)$ is the same as $f^{(n)}(y)$ in Eq. (6), and hence $g_s^{(n)}(y)$ and $f^{(n)}(y)$ are orthogonal to $f^{(0)}(y)$ and $g_s^{(0)}(y)$, respectively. Thus, if there are Yukawa couplings of the Higgs field to the doublets and singlets, e.g. $-\tilde{y}_u' \overline{Q} i\sigma_2 H^* U + \text{H.c.}$, in the effective 4D action the Higgs boson would only connect the same modes:

$$-y_u' \Big[\overline{Q}^{(0)}(x) i\sigma_2 H^{(0)*}(x) U^{(0)}(x) + \sum_{n=1}^{\infty} \overline{Q}^{(n)}(x) i\sigma_2 H^{(0)*}(x) U^{(n)}(x) \Big] + \text{H.c.} \tag{13}$$

Consequently, a mixing mass term between the zero mode of a singlet (doublet) and a KK mode of a doublet (singlet) cannot be generated by the Higgs VEV due to this orthogonality. Moreover, the Yukawa couplings between the Higgs and fermion zero modes are the same as in the SM, except for an effect due to the mixing between the Higgs and ϕ. There is no decay process of ϕ like Fig. 1. Therefore, ϕ can neither be produced from $q\overline{q}$ nor decay into quarks and leptons. This setup is not mandatory, but it forbids minor processes and maximally simplifies the analysis. For completeness, in Appendix B we give a brief discussion on the impact of the alternative assumption that the singlet Yukawa couplings to Φ are the same as the corresponding doublet Yukawa couplings.

Now we discuss how the fermion KK modes couple with the gauge fields. The zero mode of a gauge field has a flat profile, while its KK modes have profiles as

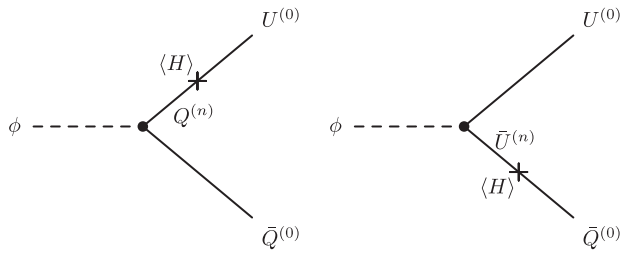

FIG. 1. Nonexistent decay $\phi \to U^{(0)} \bar{Q}^{(0)}$.

$$f_{\rm gauge}^{(n)} = \sqrt{\frac{2}{\pi R}} \cos\frac{ny}{R}. \tag{14}$$

Masses of these KK modes are $nM_{\rm KK}$, if we neglect the contributions for W and Z from the Higgs VEV. From the flat profile of the zero-mode gluon and the orthogonality between different KK modes, we can obtain the interactions between the zero-mode gluon and quarks:

$$\mathcal{L}_{g\overline{Q}Q} = g_s \sum_{n=1}^{\infty} (\overline{Q}^{(n)} \not{G} Q^{(n)} + \overline{U}^{(n)} \not{G} U^{(n)} + \overline{D}^{(n)} \not{G} D^{(n)}) + g_s (\overline{Q}_L^{(0)} \not{G} Q_L^{(0)} + \overline{U}_R^{(0)} \not{G} U_R^{(0)} + \overline{D}_R^{(0)} \not{G} D_R^{(0)}). \tag{15}$$

The interaction between the photon and fermions are similar except that the gauge coupling is replaced by the electric charge. In Appendix A, we explicitly write down the relevant Lagrangian involved in our calculation.

The Feynman diagrams for $gg \to \phi$ and $\phi \to \gamma\gamma$ are shown in Fig. 2. The effective operators of ϕGG and ϕAA couplings can be obtained by integrating out the fermion loops. This is similar to the SM Higgs case. Adopting the parametrization in Ref. [111], the effective operators are

$$\mathcal{L} \supset \kappa_g \frac{\alpha_s}{12\pi v_\phi} \phi G_{\mu\nu}^a G^{a\mu\nu} + \kappa_\gamma \frac{\alpha}{\pi v_\phi} \phi A_{\mu\nu} A^{\mu\nu}, \tag{16}$$

where the factors κ_g and κ_γ come from loop integration and are mainly contributed by fermion loops in our model:

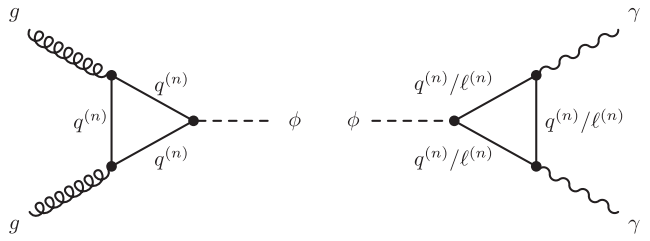

(a) $gg \to \phi$ (b) $\phi \to \gamma\gamma$

FIG. 2. Feynman diagrams for gluon-gluon fusion to ϕ (a) and $\phi \to \gamma\gamma$ decay (b) through the loops of fermion KK modes. Here $q^{(n)} = Q^{(n)}, U^{(n)}, D^{(n)}$, while $\ell^{(n)} = L^{(n)}, E^{(n)}$.

$$\kappa_g = \sum_f 2C(r_f)\kappa_f A_f(\tau_f), \tag{17}$$

$$\kappa_\gamma = \sum_f \frac{N_c(r_f)Q_f^2}{6}\kappa_f A_f(\tau_f), \tag{18}$$

where $C(r_f)$ and $N_c(r_f)$ are the index and the dimension of the $SU(3)_C$ representation where the fermion lives in, respectively. Q_f is the electric charge of the fermion. The loop function $A_f(\tau_f)$ is defined as

$$A_f(\tau_f) = \frac{3}{2\tau_f^2}[(\tau_f - 1)\arcsin^2\sqrt{\tau_f} + \tau_f] \tag{19}$$

with $\tau_f \equiv m_\phi^2/4m_f^2 \leq 1$. The factor κ_f corresponds to the $\phi\overline{F}^{(n)}F^{(n)}$ coupling

$$\mathcal{L} \supset -\kappa_f^{(n)}\frac{m_n}{v_\phi}\phi\overline{F}^{(n)}F^{(n)}. \tag{20}$$

From the action (9), we can read off the factor as

$$\kappa_f^{(n)} = \frac{y_f^2 v_\phi^2}{m_n^2}. \tag{21}$$

Combining all the results above, one can calculate the gluon-gluon fusion production cross section for ϕ and its diphoton partial decay width. Since there are three generations of fermions with different KK modes, the production rate for $pp \to \phi \to \gamma\gamma$ would be significantly increased.

III. THE KK MODES OF Φ AND SCALAR MIXING

In this section, we discuss more details about the singlet scalar Φ to justify the model.

First of all, let us show that the vacuum expectation value of the Higgs and Φ are flat under certain parameter ranges. The 5D action of the scalar sector is given by

$$S_{\text{scalar}} = \int d^4x \int_0^{\pi R} dy \left[(D^M H)^\dagger D_M H + \frac{1}{2}\partial^M\Phi\partial_M\Phi + \mu^2|H|^2 + \frac{1}{2}M^2\Phi^2 - \tilde{\lambda}|H|^4 - \frac{\tilde{\lambda}_\phi}{4!}\Phi^4 - \frac{\tilde{\lambda}_{\phi h}}{2}\Phi^2|H|^2\right], \tag{22}$$

where $\tilde{\lambda}$, $\tilde{\lambda}_\phi$, and $\tilde{\lambda}_{\phi h}$ are dimensionful couplings. Following the method used in Ref. [112], we can minimize the energy density $E = E_{\text{der}} + V(\Phi, H)$ to determine the vacuum, where

$$E_{\text{der}} = \int_0^{\pi R} dy \left[|\partial_y H|^2 + \frac{1}{2}(\partial_y\Phi)^2\right], \tag{23}$$

$$V(\Phi, H) = \int_0^{\pi R} dy \left(-\mu^2|H|^2 - \frac{1}{2}M^2\Phi^2 + \tilde{\lambda}|H|^4 + \frac{\tilde{\lambda}_\phi}{4!}\Phi^4 + \frac{\tilde{\lambda}_{\phi h}}{2}\Phi^2|H|^2\right). \tag{24}$$

We impose Neumann boundary conditions on H and Φ at both ends of the interval, and therefore H and Φ can be decomposed as

$$H(x^\mu, y) = \frac{1}{\sqrt{\pi R}}H^{(0)}(x^\mu) + \sqrt{\frac{2}{\pi R}}\sum_{n=1}^{\infty} H^{(n)}(x^\mu)\cos\left(\frac{ny}{R}\right), \tag{25}$$

$$\Phi(x^\mu, y) = \frac{1}{\sqrt{\pi R}}\phi^{(0)}(x^\mu) + \sqrt{\frac{2}{\pi R}}\sum_{n=1}^{\infty} \phi^{(n)}(x^\mu)\cos\left(\frac{ny}{R}\right). \tag{26}$$

Substituting Eqs. (25) and (26) into E_{der}, we find that

$$E_{\text{der}} = \sum_{n=1}^{\infty}\frac{n^2}{R^2}|H^{(n)}|^2 + \frac{1}{2}\sum_{n=1}^{\infty}\frac{n^2}{R^2}(\phi^{(n)})^2, \tag{27}$$

which is only contributed by $n \geq 1$ KK modes, since the zero modes have y-independent profiles. Obviously, the minimum of E_{der} is reached when $\langle H^{(n)}\rangle = 0$ and $\langle\phi^{(n)}\rangle = 0$.

The potential $V(\Phi, H)$ can be rewritten as

$$V(\Phi, H) = \int_0^{\pi R} dy \left\{\frac{\tilde{\lambda}_\phi}{4!}\left[(\Phi^2 - \tilde{v}_\phi^2) + \frac{6\tilde{\lambda}_{\phi h}}{\tilde{\lambda}_\phi}\left(|H|^2 - \frac{\tilde{v}^2}{2}\right)\right]^2 + \left(\tilde{\lambda} - \frac{3\tilde{\lambda}_{\phi h}^2}{2\tilde{\lambda}_\phi}\right)\left(|H|^2 - \frac{\tilde{v}^2}{2}\right)^2 - \frac{\tilde{\lambda}_{\phi h}}{4}\tilde{v}_\phi^2\tilde{v}^2 - \frac{\tilde{\lambda}_\phi}{24}\tilde{v}_\phi^4 - \frac{\tilde{\lambda}}{4}\tilde{v}^4\right\}, \tag{28}$$

where constants $\tilde{v}^2$ and $\tilde{v}_\phi^2$ are determined by matching the mass terms:

$$\frac{\tilde{\lambda}_{\phi h}\tilde{v}^2}{2} + \frac{\tilde{\lambda}_\phi\tilde{v}_\phi^2}{6} = M^2, \qquad \frac{\tilde{\lambda}_{\phi h}\tilde{v}_\phi^2}{2} + \tilde{\lambda}\tilde{v}^2 = \mu^2. \tag{29}$$

The solutions are

$$\tilde{v}^2 = \frac{6\tilde{\lambda}_{\phi h}M^2 - 2\tilde{\lambda}_\phi\mu^2}{3\tilde{\lambda}_{\phi h}^2 - 2\tilde{\lambda}\tilde{\lambda}_\phi}, \qquad \tilde{v}_\phi^2 = \frac{6\tilde{\lambda}_{\phi h}\mu^2 - 12\tilde{\lambda}M^2}{3\tilde{\lambda}_{\phi h}^2 - 2\tilde{\lambda}\tilde{\lambda}_\phi}. \tag{30}$$

If

$$\tilde{\lambda}_\phi > 0, \qquad \tilde{\lambda} - \frac{3\tilde{\lambda}_{\phi h}^2}{2\tilde{\lambda}_\phi} > 0, \tag{31}$$

from Eq. (28) one can find that $V(\Phi, H)$ is minimized when $|H|^2 = \tilde{v}^2/2$ and $\Phi^2 = \tilde{v}_\phi^2$. This implies that both the VEVs $\langle H\rangle$ and $\langle\Phi\rangle$ are y-independent, i.e., no $n \geq 1$ KK mode can obtain a nonzero VEV. This is the true vacuum, as it is consistent with the minimization condition of $E_{\rm der}$. The vacuum stability requires that $\tilde{\lambda}_\phi > 0$ and $\tilde{\lambda} > 0$. Therefore, if $\tilde{\lambda}_{\phi h} \ll \tilde{\lambda}_\phi, \tilde{\lambda}$, the conditions (31) would be satisfied and thus only the zero modes of H and Φ develop nonzero VEVs.

There is no mixing mass term between the zero modes and the $n \geq 1$ KK modes of H and Φ, since terms like $\langle\phi^{(0)}\rangle^2 H^{(0)\dagger} H^{(n)}$, $|\langle H^{(0)}\rangle|^2 H^{(0)\dagger} H^{(n)}$, $\langle\phi^{(0)}\rangle^2 \phi^{(0)}\phi^{(n)}$, $\langle\phi^{(0)}\rangle\langle H^{(0)\dagger}\rangle H^{(n)}\phi^{(0)}$, $|\langle H^{(0)}\rangle|^2\phi^{(0)}\phi^{(n)}$, $\mu^2 H^{(0)\dagger}H^{(n)}$, and $M^2\phi^{(0)}\phi^{(n)}$ vanish after the integration over y. Nevertheless, the mixing between the zero modes of H and Φ is inevitable. Although more data are required to increase the statistics, current LHC results suggest that the Higgs couplings to SM particles are quite consistent with the standard model. Thus it would be more safe to demand a small mixing. The 4D potential involving the zero modes $\phi^{(0)} = v + \phi$ and $H^{(0)} = (0, (v+h)/\sqrt{2})^{\rm T}$ is

$$\begin{aligned} V(H^{(0)}, \phi^{(0)}) = & -\frac{\mu^2}{2}(v+h)^2 + \frac{1}{4}\lambda(v+h)^4 \\ & - \frac{M^2}{2}(v_\phi + \phi)^2 + \frac{\lambda_\phi}{4!}(v_\phi+\phi)^4 \\ & + \frac{\lambda_{\phi h}}{4}(v+h)^2(v_\phi+\phi)^2, \end{aligned} \tag{32}$$

where the dimensionless couplings and VEVs are defined as

$$\begin{aligned} &\lambda = \frac{\tilde{\lambda}}{\pi R}, \qquad \lambda_\phi = \frac{\tilde{\lambda}_\phi}{\pi R}, \qquad \lambda_{\phi h} = \frac{\tilde{\lambda}_{\phi h}}{\pi R}, \\ &v^2 = \pi R \tilde{v}^2, \qquad v_\phi^2 = \pi R \tilde{v}_\phi^2. \end{aligned} \tag{33}$$

The minimization conditions of the potential give

$$\frac{\lambda_{\phi h} v^2}{2} + \frac{\lambda_\phi v_\phi^2}{6} = M^2, \qquad \frac{\lambda_{\phi h} v_\phi^2}{2} + \lambda v^2 = \mu^2, \tag{34}$$

which is just Eq. (29). According to the second equation, for natural values $v_\phi \sim 1$ TeV and $\lambda_{\phi h} v_\phi^2/2 \sim \mathcal{O}((100\ {\rm GeV})^2)$, a small mixing coupling $\lambda_{\phi h}$ of $\mathcal{O}(10^{-2})$ is needed. Since $\lambda \approx 0.13$ and the natural value for λ_ϕ is $\mathcal{O}(0.1) - \mathcal{O}(1)$, we have $\lambda \gg \lambda_{\phi h}$ and $\lambda_\phi \gg \lambda_{\phi h}$ as needed.

The mass matrix for h and ϕ is

$$\begin{pmatrix} m_h^2 & \lambda_{\phi h} v v_\phi \\ \lambda_{\phi h} v v_\phi & m_\phi^2 \end{pmatrix}, \tag{35}$$

where $m_h^2 = 2\lambda v^2$ and $m_\phi^2 = \lambda_\phi v_\phi^2/3$. The physical masses are given by

$$m_{h_{1,2}}^2 = \frac{1}{2}\left[m_h^2 + m_\phi^2 \mp \sqrt{(m_\phi^2 - m_h^2)^2 + 4\lambda_{h\phi}^2 v^2 v_\phi^2}\right]. \tag{36}$$

If $m_\phi^2 \gg 2\lambda_{h\phi} v v_\phi$, they are essentially decoupled, and we have $m_{h_1}^2 \approx m_h^2$ and $m_{h_2}^2 \approx m_\phi^2$.

Parametrizing the mixing matrix as

$$\begin{pmatrix} h_1 \\ h_2 \end{pmatrix} = \begin{pmatrix} \cos\alpha & -\sin\alpha \\ \sin\alpha & \cos\alpha \end{pmatrix}\begin{pmatrix} h \\ \phi \end{pmatrix}, \tag{37}$$

we can find that

$$\tan 2\alpha = \frac{2\lambda_{h\phi} v v_\phi}{m_\phi^2 - m_h^2}, \tag{38}$$

in the small α limit,

$$\sin\alpha \approx \frac{\lambda_{h\phi} v v_\phi}{m_\phi^2 - m_h^2}. \tag{39}$$

As $m_\phi \approx 750$ GeV $\approx 6 m_h$, we have

$$m_\phi^2 - m_h^2 \approx \frac{35}{6} m_h m_\phi = \frac{35}{6}\sqrt{\frac{2}{3}\lambda\lambda_\phi}\, v v_\phi.$$

Thus the small mixing condition corresponds to

$$\sin\alpha \approx \frac{6\sqrt{3}\lambda_{h\phi}}{35\sqrt{2\lambda\lambda_\phi}} \ll 1. \tag{40}$$

For instance, $\sin\alpha \approx 0.1$ needs $\lambda_{h\phi} < 0.17\sqrt{\lambda_\phi}$.

On the other hand, the value of $\lambda_{h\phi}$ also affects the tree level decay $\phi \to hh$, whose partial width is approximately given by

$$\Gamma(\phi \to hh) \approx \frac{\sqrt{2} m_\phi}{16\pi}\frac{\lambda_{h\phi}^2}{\lambda_\phi^2}. \tag{41}$$

If $\lambda_{h\phi} \sim \lambda_\phi$, we would have $\Gamma(\phi \to hh) \sim 0.03 m_\phi$. Then this channel would be dominant and give a broad total width. However, it would be easily excluded by the 8 TeV LHC result $\sigma(pp \to \phi \to hh) < 39$ fb [113]. For these reasons, below we will just consider the small mixing case and fix $\lambda_{h\phi} = 0.01$.

IV. INTERPRETATION TO THE 750 GEV DIPHOTON RESONANCE

In the model, the effective operators for ϕ couplings to gluons and photons can be explicitly expressed as

$$\mathcal{L}_{\phi gg} = \frac{\alpha_s v_\phi}{\pi}\left[\sum_{n=1}^{n_*}\frac{y_q^2 A_f(\tau_n)}{y_q^2 v_\phi^2 + n^2 M_{\rm KK}^2}\right]\phi G^a_{\mu\nu}G^{a\mu\nu}, \tag{42}$$

$$\mathcal{L}_{\phi\gamma\gamma} = \frac{\alpha}{\pi}\left[\sum_{n=1}^{n_*}\frac{5}{3}\frac{y_q^2 v_\phi A_f(\tau_q^{(n)})}{y_q^2 v_\phi^2 + n^2 M_{\rm KK}^2} + \sum_{n=1}^{n_*}\frac{y_l^2 v_\phi A_f(\tau_l^{(n)})}{y_l^2 v_\phi^2 + n^2 M_{\rm KK}^2}\right] \times \phi A_{\mu\nu}A^{\mu\nu}, \tag{43}$$

where we have included all vectorlike fermion loops, and n_* is the maximum of n we consider. Note that the model we discuss in this paper is actually an effective model, and the perturbative unitarity could be violated for a large n_*. According to the unitarity arguments in Ref. [114], we have $n < 3$ for this model. Thus we adopt $n_* = 2$ in the following calculation to obtain an optimized enhancement for the $pp \to \phi \to \gamma\gamma$ production.

The free parameters in the model are v_ϕ, $M_{\rm KK}$, y_q, and y_l. The Yukawa couplings y_q and y_l should not to be too large to remain perturbative. The ϕ decay channels involved are $\phi \to gg$, $\gamma\gamma$, hh, $Z\gamma$, ZZ, and W^+W^-. The hh channel is the only tree-level decay process and the rest are generated by vectorlike fermion loops. We numerically calculate the partial widths for the loop-induced channels using the code FeynCalc [115] and LoopTools [116].

Under the narrow width approximation, the cross section for $pp \to \phi \to X_1X_2$ can be computed by

$$\sigma(pp \to \phi \to X_1X_2) = \left(\frac{k_{gg}}{0.1}\right)^2 \sigma_{\rm ref}(pp \to \phi){\rm Br}(\phi \to X_1X_2) \tag{44}$$

with

$$k_{gg} = \frac{1\ {\rm TeV}}{M_{\rm KK}}\frac{\alpha_s v_\phi}{\pi M_{\rm KK}}\sum_{n=1}^{n_*}\frac{y_q^2 A_f(\tau_n)}{y_q^2 v_\phi^2/M_{\rm KK}^2 + n^2}, \tag{45}$$

where ${\rm Br}(\phi \to X_1X_2)$ is the branching ratio of the $\phi \to X_1X_2$ decay. We calculate $\sigma_{\rm ref}(pp \to \phi)$ using MadGraph 5 [117] and FeynRules [118], and obtain $\sigma_{\rm ref}(pp \to \phi) = 16.725(3.783)$ pb at the 13 TeV (8 TeV) LHC.

In the following, we investigate which values of the parameters can give a cross section of $pp \to \phi \to \gamma\gamma$ consistent with observation. In this model, the $\phi \to gg$ partial width is much larger than that of any other channel. Therefore we can roughly estimate the branching ratio of $\phi \to \gamma\gamma$ as

$${\rm Br}(\phi \to \gamma\gamma) \approx \frac{\Gamma(\phi \to \gamma\gamma)}{\Gamma(\phi \to gg)} = \frac{8\alpha^2}{9\alpha_s^2} \tag{46}$$

for $y_l = y_q$. Thus the cross section $\sigma(pp \to \phi \to \gamma\gamma)$ at 13 TeV is

$$\begin{aligned}\sigma(pp \to \phi \to \gamma\gamma) &\approx \frac{800\alpha^2}{9\pi^2}\sigma_{\rm ref}(pp \to \phi)\frac{v_\phi^2}{M_{\rm KK}^2} \times \left|\sum_{n=1}^{n_*}\frac{y_q^2 A_f(\tau_n)}{y_q^2 v_\phi^2/M_{\rm KK}^2 + n^2}\right|^2 \\ &\approx 9.2\ {\rm fb}\cdot\frac{v_\phi^2}{M_{\rm KK}^2}\left|\sum_{n=1}^{n_*}\frac{y_q^2 A_f(\tau_n)}{y_q^2 v_\phi^2/M_{\rm KK}^2 + n^2}\right|^2.\end{aligned} \tag{47}$$

The diphoton excess signal at the 13 TeV LHC corresponds to $\sigma(pp \to \phi \to \gamma\gamma) = 5 - 20$ fb. Apparently, if $v_\phi \sim M_{\rm KK} \sim 1$ TeV and $y_q \sim 1$, $\sigma(pp \to \phi \to \gamma\gamma)$ at 13 TeV would be around 9 fb, which is favored by current data.

On the other hand, there are some constraints for resonances from LHC Run 1 data. Relevant 95% C.L. bounds at the 8 TeV LHC include [113,119–124]

$$\sigma(pp \to \phi \to ZZ) < 12\ {\rm fb}, \tag{48}$$

$$\sigma(pp \to \phi \to W^+W^-) < 40\ {\rm fb}, \tag{49}$$

$$\sigma(pp \to \phi \to Z\gamma) < 4\ {\rm fb}, \tag{50}$$

$$\sigma(pp \to \phi \to jj) < 2.5\ {\rm pb}, \tag{51}$$

$$\sigma(pp \to \phi \to hh) < 39\ {\rm fb}. \tag{52}$$

In the model, ϕ could decay into SM quarks and leptons through the mixing with the Higgs boson. However, since we have chosen a very small mixing parameter, these decay channels can be neglected. Therefore, the $pp \to \phi \to jj$ process principally comes from the $\phi \to gg$ decay, and the $pp \to \phi \to l^+l^-$ process is irrelevant to the phenomenology here.

Figure 3 shows the branching ratios of ϕ decay channels as functions of y_l, where the other parameters are fixed as $v_\phi = M_{\rm KK} = 1$ TeV and $y_q = 1$. We can find that the gg channel is dominant, with a branching ratio larger than the subdominant channels W^+W^- and ZZ by about 2 orders of magnitude. The diphoton channel has a branching ratio of $\sim\mathcal{O}(10^{-3})$, increasing as y_l increases. The γZ channel is the least important.

After calculation, it turns out that the $pp \to \phi \to jj$, $Z\gamma$, and hh searches at the 8 TeV LHC can hardly constrain the relevant region of the parameter space. Note that although the ϕgg coupling is dramatically enhanced by loops of fermion KK modes, the 8 TeV bound from the dijet channel

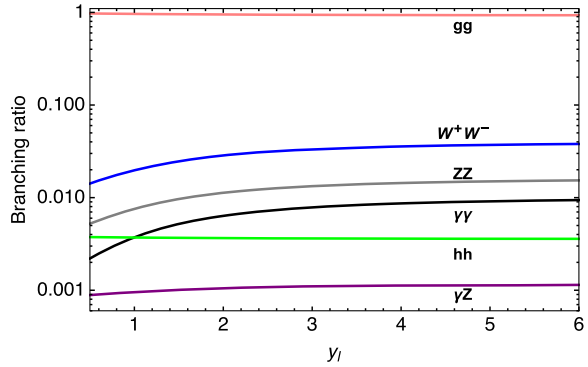

FIG. 3. Branching ratios of ϕ decay channels as functions of y_l for $v_\phi = M_{\rm KK} = 1$ TeV and $y_q = 1$.

is still quite weak. For instance, assuming a moderate value of $\mathrm{BR}(\phi \to \gamma\gamma) = 0.004$, for $\sigma(pp \to \phi \to \gamma\gamma) = 5$–$20$ fb at 13 TeV, the $pp \to \phi \to gg$ cross section at 8 TeV can be estimated as

$$\sigma^{8\ \mathrm{TeV}}(pp \to \phi \to gg) = \frac{\sigma^{8\ \mathrm{TeV}}_{\rm ref}(pp \to \phi)}{\sigma^{13\ \mathrm{TeV}}_{\rm ref}(pp \to \phi)} \sigma^{13\ \mathrm{TeV}} \times (pp \to \phi \to \gamma\gamma) \frac{\mathrm{Br}(\phi \to gg)}{\mathrm{Br}(\phi \to \gamma\gamma)} \approx 0.3\text{–}1.1\ \mathrm{pb}, \quad (53)$$

which is well below the 95% C.L. upper limit 2.5 pb from the 8 TeV dijet resonance search.

Figure 4 shows the contours of $\sigma_{\gamma\gamma} \equiv \sigma(pp \to \phi \to \gamma\gamma)$ at 13 TeV in the $v_\phi - y_{q,l}$ plane for $M_{\rm KK} = 1$ TeV assuming $y_l = y_q$. We can see that $\sigma_{\gamma\gamma} = 5$–$20$ fb

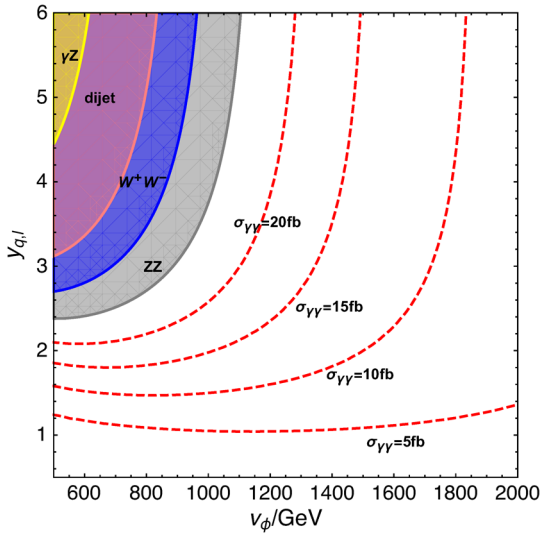

FIG. 4. Contours of $\sigma_{\gamma\gamma}$ (red dashed lines) at 13 TeV in the $v_\phi - y_{q,l}$ plane for $M_{\rm KK} = 1$ TeV assuming $y_l = y_q$. The gray, blue, pink, and yellow regions are excluded at 95% C.L. by the $pp \to \phi \to ZZ, W^+W^-$, dijet, and γZ searches at the 8 TeV LHC.

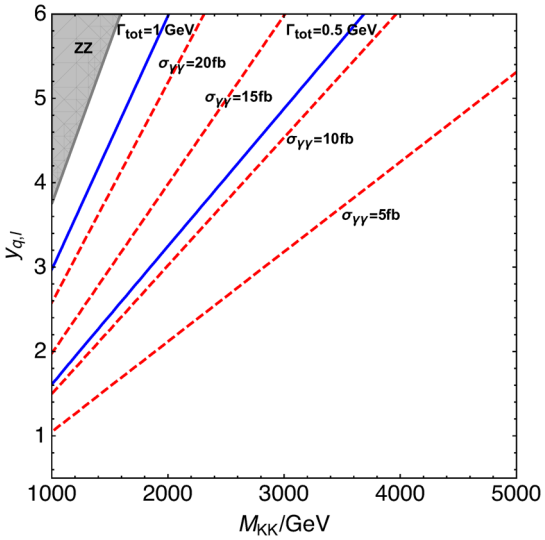

FIG. 5. Contours of $\sigma_{\gamma\gamma}$ (red dashed lines) at 13 TeV and the total width of ϕ (blue solid lines) in the $M_{\rm KK} - y_{q,l}$ plane for $v_\phi = 1$ TeV assuming $y_l = y_q$. The gray region is excluded at 95% C.L. by the $pp \to \phi \to ZZ$ search at the 8 TeV LHC.

corresponds to a large region that is not excluded by the 8 TeV LHC searches for the $pp \to \phi \to ZZ$, W^+W^-, dijet, and γZ processes. This means that our interpretation to the diphoton excess is consistent with the 8 TeV LHC data, although a large $y_{q,l} \gtrsim 1$ is demanded to give a sufficiently large $\sigma_{\gamma\gamma}$. A smaller v_ϕ would decrease the masses of vectorlike fermions in loops, and hence increase the signal.

In order to investigate how large $M_{\rm KK}$ could be, we fix $v_\phi = 1$ TeV and demonstrate in Fig. 5 the contours of $\sigma_{\gamma\gamma}$

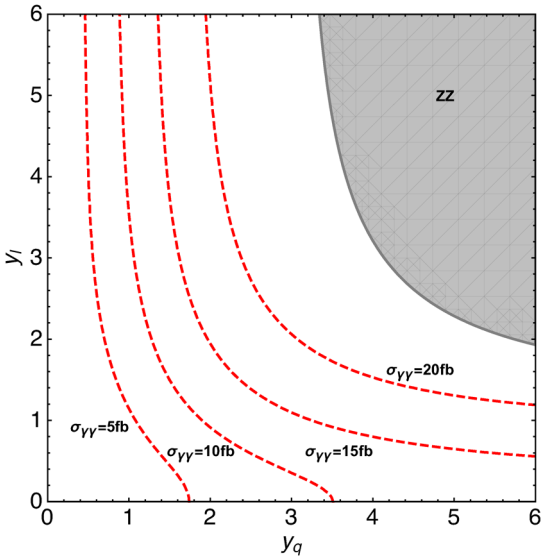

FIG. 6. Contours of $\sigma_{\gamma\gamma}$ (red dashed lines) at 13 TeV in the $y_q - y_l$ plane for $M_{\rm KK} = v_\phi = 1$ TeV. The gray region is excluded at 95% C.L. by the $pp \to \phi \to ZZ$ search at the 8 TeV LHC.

in the $M_{\rm KK} - y_{q,l}$ plane assuming $y_l = y_q$. We find that if we can tolerate $y_{q,l}$ as large as 5.3, $M_{\rm KK}$ can reach up to 5 TeV for an desired diphoton signal. On the other hand, if we can just tolerate $y_{q,l} \sim 2$, then $M_{\rm KK}$ is bounded to below 2 TeV. We also plot the contours of the ϕ total decay width $\Gamma_{\rm tot}$ in Fig. 5. We find that the predicted $\Gamma_{\rm tot}$ could reach up to $\sim$1 GeV, which is still smaller than the favored value 45 GeV from the preliminary ATLAS analysis. If such a broad width persists in the follow-up experiments, extra decay channels might be needed to increase the total width. For instance, ϕ may decay into a pair of DM particles and this can be still consistent the 8 TeV bounds [4,66].

Finally, we study how $\sigma_{\gamma\gamma}$ depends on y_q and y_l, as presented in Fig. 6, where $M_{\rm KK} = v_\phi = 1$ TeV is fixed. Since vectorlike quark KK modes both enter the ϕgg and $\phi\gamma\gamma$ effective couplings while vectorlike charged lepton KK modes only contribute to the $\phi\gamma\gamma$ effective coupling, $\sigma_{\gamma\gamma}$ is more sensitive to y_q. As y_q decreases, y_l should be dramatically increased to enhance the $\gamma\gamma$ branching ratio for compensating the signal. Although y_l may be even allowed to vanish, y_q should be at least $\sim$0.5 for explaining the diphoton excess.

V. CONCLUSIONS AND DISCUSSIONS

The 750 GeV diphoton excess recently found in the 13 TeV LHC data have drawn great attention of the high energy physics community. In this work, we interpret it as a singlet scalar ϕ in an extra dimensional model, where just one compactified extra dimension is introduced.

We assume there is a 5D singlet scalar field Φ coupled to multiple vectorlike 5D fermions through Yukawa interactions. After Φ gets a VEV, its zero-mode excitation around the VEV becomes the observed scalar ϕ, and the 5D fermions acquire bulk mass terms, which localize the zero modes of these fermions. By imposing appropriate boundary conditions, the fermion zero modes become chiral and play the roles of ordinary SM fermions, while the KK modes remain vectorlike. ϕ can mix with the SM Higgs boson. However, after considering the LHC measurement of the Higgs couplings as well as the natural choices of model parameters, a small mixing case is favored.

The vectorlike fermion KK modes have the same gauge quantum numbers as the corresponding zero modes. As ϕ couples them, they can induce significantly large ϕgg and $\phi\gamma\gamma$ effective couplings through loop diagrams. Consequently, this model can easily give an observed cross section of $\mathcal{O}(10)$ fb for the diphoton excess without contradicting the 8 TeV LHC constraints.

Since the decay channels $\phi \to gg$, ZZ, $Z\gamma$, and W^+W^- always exist along with the diphoton channel in this model, follow-up experimental searches for ϕ through these final states would be crucial to test the model. On the other hand, if the vectorlike quark KK modes have masses of $\sim\mathcal{O}(1)$ TeV, they could be accessible at the 13 TeV and 14 TeV LHC. Once produced, they can decay into ϕ and the corresponding zero-mode quarks and may lead to distinguishable signatures. If they are heavier, say $\sim\mathcal{O}(10)$ TeV, it would become a task for future higher energy hadron colliders, such as SppC and FCC-hh.

ACKNOWLEDGMENTS

This work is supported by the National Natural Science Foundation of China (NSFC) under Grants No. 11375277, No. 11410301005, and No. 11005163, the Fundamental Research Funds for the Central Universities, and the Sun Yat-Sen University Science Foundation. ZHY is supported by the Australian Research Council.

APPENDIX A: RELEVANT INTERACTION LAGRANGIANS

The interaction Lagrangians relevant to the calculation are listed below.

$\phi\overline{F}^{(n)}F^{(n)}$ interactions:

$$\begin{aligned}\mathcal{L}_{\phi FF} = &-y_q \frac{M_q}{\sqrt{M_q^2 + n^2 M_{\rm KK}^2}} \phi \Big[\overline{u}_2^{(n)} u_2^{(n)} + \overline{d}_2^{(n)} d_2^{(n)} \\ &+ \overline{u}_1^{(n)} u_1^{(n)} + \overline{d}_1^{(n)} d_1^{(n)}\Big] - y_l \frac{M_l}{\sqrt{M_l^2 + n^2 M_{\rm KK}^2}} \\ &\times \phi[\overline{\nu}_2^{(n)} \nu_2^{(n)} + \overline{e}_2^{(n)} e_2^{(n)} + \overline{e}_1^{(n)} e_1^{(n)}]. \end{aligned} \tag{A1}$$

$A\overline{F}^{(n)}F^{(n)}$ interactions:

$$\begin{aligned}\mathcal{L}_{AFF} = eA_\mu \Big[&\frac{2}{3}\overline{u}_2^{(n)}\gamma^\mu u_2^{(n)} - \frac{1}{3}\overline{d}_2^{(n)}\gamma^\mu d_2^{(n)} + \frac{2}{3}\overline{u}_1^{(n)}\gamma^\mu u_1^{(n)} \\ &- \frac{1}{3}\overline{d}_1^{(n)}\gamma^\mu d_1^{(n)} - \overline{e}_2^{(n)}\gamma^\mu e_2^{(n)} - \overline{e}_1^{(n)}\gamma^\mu e_1^{(n)}\Big]. \end{aligned} \tag{A2}$$

$Z\overline{F}^{(n)}F^{(n)}$ interactions:

$$\begin{aligned}\mathcal{L}_{ZFF} = \frac{g_2}{2c_W} Z_\mu \Big[&\left(1 - \frac{4}{3}s_W^2\right)\overline{u}_2^{(n)}\gamma^\mu u_2^{(n)} \\ &- \left(1 - \frac{2}{3}s_W^2\right)\overline{d}_2^{(n)}\gamma^\mu d_2^{(n)} - \frac{4}{3}s_W^2\overline{u}_1^{(n)}\gamma^\mu u_1^{(n)} \\ &+ \frac{2}{3}s_W^2\overline{d}_1^{(n)}\gamma^\mu d_1^{(n)} + \overline{\nu}_2^{(n)}\gamma^\mu \nu_2^{(n)} \\ &- (1 - 2s_W^2)\overline{e}_2^{(n)}\gamma^\mu e_2^{(n)} + 2s_W^2\overline{e}_1^{(n)}\gamma^\mu e_1^{(n)}\Big]. \end{aligned} \tag{A3}$$

$W\overline{F}^{(n)}F'^{(n)}$ interactions:

$$\begin{aligned}\mathcal{L}_{WFF'} = \frac{g_2}{\sqrt{2}}[&W_\mu^+ \overline{u}_2^{(n)}\gamma^\mu d_2^{(n)} + W_\mu^- \overline{d}_2^{(n)}\gamma^\mu u_2^{(n)} \\ &+ W_\mu^+ \overline{\nu}_2^{(n)}\gamma^\mu e_2^{(n)} + W_\mu^- \overline{\nu}_2^{(n)}\gamma^\mu e_2^{(n)}]. \end{aligned} \tag{A4}$$

$G\overline{F}^{(n)}F^{(n)}$ interactions:

$$\mathcal{L}_{GFF} = g_s G_\mu^a [\overline{u}_2^{(n)}\lambda^a\gamma^\mu u_2^{(n)} + \overline{d}_2^{(n)}\lambda^a\gamma^\mu d_2^{(n)} + \overline{u}_1^{(n)}\lambda^a\gamma^\mu u_1^{(n)} + \overline{d}_1^{(n)}\lambda^a\gamma^\mu d_1^{(n)}]. \quad \text{(A5)}$$

λ^a denote the Gell-Mann matrices. Note that the subscripts 1 and 2 denote the fermion coming from a singlet and a doublet, respectively. That is to say, $Q = (u_2, d_2)^{\mathrm{T}}$, $U = u_1$, $D = d_1$, $L = (\nu_2, e_2)^{\mathrm{T}}$, and $E = e_1$. Remember that there are three generations of fermions.

APPENDIX B: AN ALTERNATIVE SETUP OF YUKAWA COUPLINGS

In this appendix, we discuss an alternative setup that the singlet Yukawa couplings to Φ are the same as the corresponding doublet Yukawa couplings. The profiles of a singlet fermion field become

$$f_s^{(n)}(y) = \sqrt{\frac{2}{\pi R}}\sin\frac{ny}{R}, \quad \text{(B1)}$$

$$g_s^{(0)}(y) = \sqrt{\frac{2M_f}{1-e^{-2\pi M_f R}}}e^{-M_f y}, \quad \text{(B2)}$$

$$g_s^{(n)}(y) = \sqrt{\frac{2/\pi R}{M_f^2 + n^2/R^2}}\left(-\frac{n}{R}\cos\frac{ny}{R} + M_f\sin\frac{ny}{R}\right), \quad \text{(B3)}$$

while a doublet keeps the original profiles:

$$f_d^{(0)}(y) = \sqrt{\frac{2M_f}{e^{2\pi M_f R}-1}}e^{M_f y}, \quad \text{(B4)}$$

$$f_d^{(n)}(y) = \sqrt{\frac{2/\pi R}{M_f^2 + n^2/R^2}}\left(\frac{n}{R}\cos\frac{ny}{R} + M_f\sin\frac{ny}{R}\right), \quad \text{(B5)}$$

$$g_d^{(n)}(y) = \sqrt{\frac{2}{\pi R}}\sin\frac{ny}{R}. \quad \text{(B6)}$$

Now $g_s^{(n)}(y)$ ($f_d^{(n)}(y)$) is not orthogonal to $f_d^{(0)}(y)$ ($g_s^{(0)}(y)$). The Yukawa interactions like $-\tilde{y}'_u\overline{Q}i\sigma_2 H^* U +$ H.c. lead to the following 4D Lagrangian:

$$\mathcal{L}_{\mathrm{yuk}} \supset -\frac{y'_u}{\sqrt{2}}\frac{2\pi M_q/M_{\mathrm{KK}}}{e^{\pi M_q/M_{\mathrm{KK}}} - e^{-\pi M_q/M_{\mathrm{KK}}}}(v+h)\overline{u}_2^{(0)}u_R^{(0)} - \frac{y'_u}{\sqrt{2\pi}}(v+h)\sum_{n=1}^{n_*}\frac{4(nM_qM_{\mathrm{KK}})^{3/2}}{\sqrt{n}(M_q^2+n^2M_{\mathrm{KK}}^2)^{3/2}} \times\frac{1-\cos(n\pi)e^{-\pi M_q/M_{\mathrm{KK}}}}{\sqrt{1-e^{-2\pi M_q/M_{\mathrm{KK}}}}}\overline{u}_2^{(n)}u_R^{(0)} + \mathrm{H.c.} \quad \text{(B7)}$$

The second line are mixing mass terms between the zero mode of the singlet and KK modes of the doublet. Consequently, Feynman diagrams like Fig. 1 exist, leading to ϕ decays into SM fermion pairs, where $\phi \to t\bar{t}$ is dominant.

The physical masses of the quarks can be found after diagonalizing the mass matrices. The masses of the SM-like quarks, which are the lightest ones, are given by $m_q^2 \approx m_{q,0}^2 + m_{D,1}^2 + m_{D,2}^2 + \cdots$ with

$$m_{q,0} = \frac{y'_u}{\sqrt{2}}\frac{2\pi M_q/M_{\mathrm{KK}}}{e^{\pi M_q/M_{\mathrm{KK}}} - e^{-\pi M_q/M_{\mathrm{KK}}}}v, \quad \text{(B8)}$$

$$m_{D,n} = \frac{y'_u}{\sqrt{2\pi}}\frac{4(nM_qM_{\mathrm{KK}})^{3/2}}{\sqrt{n}(M_q^2+n^2M_{\mathrm{KK}}^2)^{3/2}} \times\frac{1-\cos(n\pi)e^{-\pi M_q/M_{\mathrm{KK}}}}{\sqrt{1-e^{-2\pi M_q/M_{\mathrm{KK}}}}}v. \quad \text{(B9)}$$

For a large M_q/M_{KK}, $m_{q,0}$ is exponentially suppressed and much smaller than $m_{D,1}$, which is just power suppressed. Thus, m_q is dominated by $m_{D,n}$. Matching m_q with the observed values, we will find that the Yukawa couplings of the quark zero modes with the Higgs boson are significantly suppressed. For instance, Fig. 5 implies that in order to obtain a proper diphoton cross section $\sigma_{\gamma\gamma} \sim 10$ fb, M_q/M_{KK} should be ~ 2, leading to a Yukawa coupling of $y_{hqq} = m_{q,0}/v \approx 0.03 y_{hqq}^{\mathrm{SM}}$. The top Yukawa coupling with such a small value would be incompatible with the current measurement, as it greatly reduces the Higgs production via gluon-gluon fusion. Therefore, this setup is problematic.

[1] ATLAS Collaboration, Search for resonances decaying to photon pairs in 3.2 fb^{-1} of pp collisions at $\sqrt{s} = 13$ TeV with the ATLAS detector, Report No. ATLAS-CONF-2015-081.

[2] CMS Collaboration, Search for new physics in high mass diphoton events in proton-proton collisions at 13 TeV, Report No. CMS-PAS-EXO-15-004.

[3] K. Harigaya and Y. Nomura, Composite models for the 750 GeV diphoton excess, Phys. Lett. B **754**, 151 (2016).

[4] Y. Mambrini, G. Arcadi, and A. Djouadi, The LHC diphoton resonance and dark matter, Phys. Lett. B **755**, 426 (2016).

[5] M. Backovic, A. Mariotti, and D. Redigolo, Di-photon excess illuminates dark matter, J. High Energy Phys. 03 (2016) 157.

[6] A. Angelescu, A. Djouadi, and G. Moreau, Scenarii for interpretations of the LHC diphoton excess: Two Higgs doublets and vectorlike quarks and leptons, Phys. Lett. B **756**, 126 (2016).

[7] Y. Nakai, R. Sato, and K. Tobioka, Footprints of new strong dynamics via anomaly, arXiv:1512.04924.

[8] S. Knapen, T. Melia, M. Papucci, and K. Zurek, Rays of light from the LHC, Phys. Rev. D **93**, 075020 (2016).

[9] D. Buttazzo, A. Greljo, and D. Marzocca, Knocking on new physics' door with a scalar resonance, Eur. Phys. J. C **76**, 116 (2016).

[10] A. Pilaftsis, Diphoton signatures from heavy axion decays at LHC, Phys. Rev. D **93**, 015017 (2016).

[11] R. Franceschini, G. F. Giudice, J. F. Kamenik, M. McCullough, A. Pomarol, R. Rattazzi, M. Redi, F. Riva, A. Strumia, and R. Torre, What is the gamma gamma resonance at 750 GeV?, J. High Energy Phys. 03 (2016) 144.

[12] S. Di Chiara, L. Marzola, and M. Raidal, First interpretation of the 750 GeV di-photon resonance at the LHC, arXiv:1512.04939.

[13] S. D. McDermott, P. Meade, and H. Ramani, Singlet scalar resonances and the diphoton excess, Phys. Lett. B **755**, 353 (2016).

[14] J. Ellis, S. A. R. Ellis, J. Quevillon, V. Sanz, and T. You, On the interpretation of a possible ~750 GeV particle decaying into $\gamma\gamma$, J. High Energy Phys. 03 (2016) 176.

[15] M. Low, A. Tesi, and L.-T. Wang, A pseudoscalar decaying to photon pairs in the early LHC run 2 data, J. High Energy Phys. 03 (2016) 108.

[16] B. Bellazzini, R. Franceschini, F. Sala, and J. Serra, Goldstones in diphotons, arXiv:1512.05330.

[17] R. S. Gupta, S. Jger, Y. Kats, G. Perez, and E. Stamou, Interpreting a 750 GeV diphoton resonance, arXiv:1512.05332.

[18] C. Petersson and R. Torre, 750 GeV Diphoton Excess from the Goldstino Superpartner, Phys. Rev. Lett. **116**, 151804 (2016).

[19] E. Molinaro, F. Sannino, and N. Vignaroli, Minimal composite dynamics versus axion origin of the diphoton excess, arXiv:1512.05334.

[20] B. Dutta, Y. Gao, T. Ghosh, I. Gogoladze, and T. Li, Interpretation of the diphoton excess at CMS and ATLAS, Phys. Rev. D **93**, 055032 (2016).

[21] Q.-H. Cao, Y. Liu, K.-P. Xie, B. Yan, and D.-M. Zhang, A boost test of anomalous diphoton resonance at the LHC, arXiv:1512.05542.

[22] S. Matsuzaki and K. Yamawaki, 750 GeV diphoton signal from one-family walking technipion, arXiv:1512.05564.

[23] A. Kobakhidze, F. Wang, L. Wu, J. M. Yang, and M. Zhang, LHC 750 GeV diphoton resonance explained as a heavy scalar in top-seesaw model, arXiv:1512.05585.

[24] R. Martinez, F. Ochoa, and C. F. Sierra, Diphoton decay for a 750 GeV scalar boson in an $U(1)'$ model, arXiv:1512.05617.

[25] P. Cox, A. D. Medina, T. S. Ray, and A. Spray, Diphoton excess at 750 GeV from a radion in the bulk-Higgs scenario, arXiv:1512.05618.

[26] D. Becirevic, E. Bertuzzo, O. Sumensari, and R. Z. Funchal, Can the new resonance at LHC be a CP-Ood Higgs boson?, arXiv:1512.05623.

[27] J. M. No, V. Sanz, and J. Setford, See-saw composite Higgses at the LHC: Linking naturalness to the 750 GeV di-photon resonance, arXiv:1512.05700.

[28] S. V. Demidov and D. S. Gorbunov, On sgoldstino interpretation of the diphoton excess, arXiv:1512.05723.

[29] W. Chao, R. Huo, and J.-H. Yu, The minimal scalar-stealth top interpretation of the diphoton excess, arXiv:1512.05738.

[30] S. Fichet, G. von Gersdorff, and C. Royon, Scattering light by light at 750 GeV at the LHC, arXiv:1512.05751 [Phys. Rev. D (to be published)].

[31] D. Curtin and C. B. Verhaaren, Quirky explanations for the diphoton excess, Phys. Rev. D **93**, 055011 (2016).

[32] L. Bian, N. Chen, D. Liu, and J. Shu, A hidden confining world on the 750 GeV diphoton excess, arXiv:1512.05759.

[33] J. Chakrabortty, A. Choudhury, P. Ghosh, S. Mondal, and T. Srivastava, Di-photon resonance around 750 GeV: shedding light on the theory underneath, arXiv:1512.05767.

[34] A. Ahmed, B. M. Dillon, B. Grzadkowski, J. F. Gunion, and Y. Jiang, Higgs-radion interpretation of 750 GeV di-photon excess at the LHC, arXiv:1512.05771.

[35] P. Agrawal, J. Fan, B. Heidenreich, M. Reece, and M. Strassler, Experimental considerations motivated by the diphoton excess at the LHC, arXiv:1512.05775.

[36] C. Csaki, J. Hubisz, and J. Terning, Minimal model of a diphoton resonance: Production without gluon couplings, Phys. Rev. D **93**, 035002 (2016).

[37] A. Falkowski, O. Slone, and T. Volansky, Phenomenology of a 750 GeV Singlet, J. High Energy Phys. 02 (2016) 152.

[38] D. Aloni, K. Blum, A. Dery, A. Efrati, and Y. Nir, On a possible large width 750 GeV diphoton resonance at ATLAS and CMS, arXiv:1512.05778.

[39] Y. Bai, J. Berger, and R. Lu, A 750 GeV dark pion: Cousin of a dark G-parity-odd WIMP, arXiv:1512.05779 [Phys. Rev. D (to be published)].

[40] S. Ghosh, A. Kundu, and S. Ray, On the potential of a singlet scalar enhanced standard model, arXiv:1512.05786.

[41] E. Gabrielli, K. Kannike, B. Mele, M. Raidal, C. Spethmann, and H. Veerme, A SUSY inspired simplified model for the 750 GeV diphoton excess, Phys. Lett. B **756**, 36 (2016).

[42] R. Benbrik, C.-H. Chen, and T. Nomura, Higgs singlet as a diphoton resonance in a vectorlike quark model, Phys. Rev. D **93**, 055034 (2016).
[43] J. S. Kim, J. Reuter, K. Rolbiecki, and R. R. de Austri, A resonance without resonance: Scrutinizing the diphoton excess at 750 GeV, Phys. Lett. B **755**, 403 (2016).
[44] A. Alves, A. G. Dias, and K. Sinha, The 750 GeV *S*-cion: Where else should we look for it?, Phys. Lett. B **757**, 39 (2016).
[45] E. Megias, O. Pujolas, and M. Quiros, On dilatons and the LHC diphoton excess, arXiv:1512.06106.
[46] L. M. Carpenter, R. Colburn, and J. Goodman, Supersoft SUSY models and the 750 GeV diphoton excess, beyond effective operators, arXiv:1512.06107.
[47] J. Bernon and C. Smith, Could the width of the diphoton anomaly signal a three-body decay?, arXiv:1512.06113.
[48] W. Chao, Symmetries behind the 750 GeV diphoton excess, arXiv:1512.06297.
[49] M. T. Arun and P. Saha, Gravitons in multiply warped scenarios—at 750 GeV and beyond, arXiv:1512.06335.
[50] C. Han, H. M. Lee, M. Park, and V. Sanz, The diphoton resonance as a gravity mediator of dark matter, Phys. Lett. B **755**, 371 (2016).
[51] S. Chang, Simple $U(1)$ gauge theory explanation of the diphoton excess, Phys. Rev. D **93**, 055016 (2016).
[52] A. Ringwald and K. Saikawa, Accion dark matter in the post-inflationary Peccei-Quinn symmetry breaking scenario, arXiv:1512.06436 [Phys. Rev. D (to be published)].
[53] I. Chakraborty and A. Kundu, Diphoton excess at 750 GeV: Singlet scalars confront naturalness, Phys. Rev. D **93**, 055003 (2016).
[54] R. Ding, L. Huang, T. Li, and B. Zhu, Interpreting 750 GeV diphoton excess with R-parity violation supersymmetry, arXiv:1512.06560.
[55] H. Han, S. Wang, and S. Zheng, Scalar explanation of diphoton excess at LHC, arXiv:1512.06562.
[56] H. Hatanaka, Oblique corrections from less-Higgsless models in warped space, arXiv:1512.06595.
[57] M.-x. Luo, K. Wang, T. Xu, L. Zhang, and G. Zhu, Squarkonium/diquarkonium and the diphoton excess, Phys. Rev. D **93**, 055042 (2016).
[58] J. Chang, K. Cheung, and C.-T. Lu, Interpreting the 750 GeV diphoton resonance using photon-jets in hidden-valley-like models, Phys. Rev. D **93**, 075013 (2016).
[59] D. Bardhan, D. Bhatia, A. Chakraborty, U. Maitra, S. Raychaudhuri, and T. Samui, Radion candidate for the LHC diphoton resonance, arXiv:1512.06674.
[60] T.-F. Feng, X.-Q. Li, H.-B. Zhang, and S.-M. Zhao, The LHC 750 GeV diphoton excess in supersymmetry with gauged baryon and lepton numbers, arXiv:1512.06696.
[61] O. Antipin, M. Mojaza, and F. Sannino, A natural Coleman-Weinberg theory explains the diphoton excess, arXiv:1512.06708.
[62] F. Wang, L. Wu, J. M. Yang, and M. Zhang, 750 GeV diphoton resonance, 125 GeV Higgs and muon g-2 anomaly in deflected anomaly mediation SUSY breaking scenario, arXiv:1512.06715.
[63] J. Cao, C. Han, L. Shang, W. Su, J. M. Yang, and Y. Zhang, Interpreting the 750 GeV diphoton excess by the singlet extension of the Manohar-Wise model, Phys. Lett. B **755**, 456 (2016).
[64] F. P. Huang, C. S. Li, Z. L. Liu, and Y. Wang, 750 GeV diphoton excess from cascade decay, arXiv:1512.06732.
[65] M. Dhuria and G. Goswami, Perturbativity, vacuum stability and inflation in the light of 750 GeV diphoton excess, arXiv:1512.06782.
[66] X.-J. Bi, Q.-F. Xiang, P.-F. Yin, and Z.-H. Yu, The 750 GeV diphoton excess at the LHC and dark matter constraints, arXiv:1512.06787.
[67] J. S. Kim, K. Rolbiecki, and R. R. de Austri, Model-independent combination of diphoton constraints at 750 GeV, arXiv:1512.06797.
[68] L. Berthier, J. M. Cline, W. Shepherd, and M. Trott, Effective interpretations of a diphoton excess, arXiv:1512.06799.
[69] J. M. Cline and Z. Liu, LHC diphotons from electroweakly pair-produced composite pseudoscalars, arXiv:1512.06827.
[70] M. Chala, M. Duerr, F. Kahlhoefer, and K. Schmidt-Hoberg, Tricking Landau-Yang: How to obtain the diphoton excess from a vector resonance, Phys. Lett. B **755**, 145 (2016).
[71] K. Kulkarni, Extension of νMSM model and possible explanations of recent astronomical and collider observations, arXiv:1512.06836.
[72] D. Barducci, A. Goudelis, S. Kulkarni, and D. Sengupta, One jet to rule them all: Monojet constraints and invisible decays of a 750 GeV diphoton resonance, arXiv:1512.06842.
[73] S. M. Boucenna, S. Morisi, and A. Vicente, The LHC diphoton resonance from gauge symmetry, arXiv:1512.06878.
[74] C. W. Murphy, Vector leptoquarks and the 750 GeV diphoton resonance at the LHC, Phys. Lett. B **757**, 192 (2016).
[75] A. E. C. Hernndez and I. Nisandzic, LHC diphoton 750 GeV resonance as an indication of $SU(3)_c \times SU(3)_L \times U(1)_X$ gauge symmetry, arXiv:1512.07165.
[76] U. K. Dey, S. Mohanty, and G. Tomar, 750 GeV resonance in the dark left-right model, Phys. Lett. B **756**, 384 (2016).
[77] G. M. Pelaggi, A. Strumia, and E. Vigiani, Trinification can explain the di-photon and di-boson LHC anomalies, J. High Energy Phys. 03 (2016) 025.
[78] P. S. B. Dev and D. Teresi, Asymmetric dark matter in the sun and the diphoton excess at the LHC, arXiv:1512.07243.
[79] W.-C. Huang, Y.-L. S. Tsai, and T.-C. Yuan, Gauged two Higgs doublet model confronts the LHC 750 GeV diphoton anomaly, arXiv:1512.07268.
[80] M. Chabab, M. Capdequi-Peyranre, and L. Rahili, Naturalness in type II seesaw model and implications for physical scalars, arXiv:1512.07280.
[81] S. Moretti and K. Yagyu, The 750 GeV diphoton excess and its explanation in 2-Higgs doublet models with a real inert scalar multiplet, Phys. Rev. D **93**, 055043 (2016).
[82] K. M. Patel and P. Sharma, Interpreting 750 GeV diphoton excess in SU(5) grand unified theory, Phys. Lett. B, doi:10.1016/j.physletb.2016.04.006 (2016).
[83] M. Badziak, Interpreting the 750 GeV diphoton excess in minimal extensions of two-Higgs-doublet models, arXiv:1512.07497.
[84] S. Chakraborty, A. Chakraborty, and S. Raychaudhuri, Diphoton resonance at 750 GeV in the broken MRSSM, arXiv:1512.07527.

[85] Q.-H. Cao, S.-L. Chen, and P.-H. Gu, Strong *CP* problem, neutrino masses and the 750 GeV diphoton resonance, arXiv:1512.07541.
[86] M. Cveti, J. Halverson, and P. Langacker, String consistency, heavy exotics, and the 750 GeV diphoton excess at the LHC, arXiv:1512.07622.
[87] J. Gu and Z. Liu, Running after diphoton, Phys. Rev. D **93**, 075006 (2016).
[88] B. C. Allanach, P. S. B. Dev, S. A. Renner, and K. Sakurai, Di-photon excess explained by a resonant sneutrino in R-parity violating supersymmetry, arXiv:1512.07645.
[89] H. Davoudiasl and C. Zhang, 750 GeV messenger of dark conformal symmetry breaking, Phys. Rev. D **93**, 055006 (2016).
[90] K. Das and S. K. Rai, The 750 GeV diphoton excess in a $U(1)$ hidden symmetry model, arXiv:1512.07789.
[91] K. Cheung, P. Ko, J. S. Lee, J. Park, and P.-Y. Tseng, A Higgcision study on the 750 GeV di-photon resonance and 125 GeV SM Higgs boson with the Higgs-singlet mixing, arXiv:1512.07853.
[92] J. Liu, X.-P. Wang, and W. Xue, LHC diphoton excess from colorful resonances, arXiv:1512.07885.
[93] J. Zhang and S. Zhou, Electroweak vacuum stability and diphoton excess at 750 GeV, arXiv:1512.07889.
[94] J. A. Casas, J. R. Espinosa, and J. M. Moreno, The 750 GeV diphoton excess as a first light on supersymmetry breaking, arXiv:1512.07895.
[95] L. J. Hall, K. Harigaya, and Y. Nomura, 750 GeV diphotons: Implications for supersymmetric unification, J. High Energy Phys. 03 (2016) 017.
[96] J. de Blas, J. Santiago, and R. Vega-Morales, New vector bosons and the diphoton excess, arXiv:1512.07229.
[97] J. J. Heckman, 750 GeV Diphotons from a D3-brane, Nucl. Phys. **B906**, 231 (2016).
[98] Y. Hamada, T. Noumi, S. Sun, and G. Shiu, An O(750) GeV resonance and inflation, arXiv:1512.08984.
[99] A. Salvio and A. Mazumdar, Higgs stability and the 750 GeV diphoton excess, Phys. Lett. B **755**, 469 (2016).
[100] L. D. Landau, 65-On the angular momentum of a system of two photons, in *Collected Papers of L.D. Landau*, edited by D. T. Haar (Elsevier, Pergamon, 1965), Vol. 60, pp. 471–473.
[101] C.-N. Yang, Selection rules for the dematerialization of a particle into two photons, Phys. Rev. **77**, 242 (1950).
[102] W. S. Cho, D. Kim, K. Kong, S. H. Lim, K. T. Matchev, J.-C. Park, and M. Park, 750 GeV Diphoton Excess May Not Imply a 750 GeV Resonance, Phys. Rev. Lett. **116**, 151805 (2016).
[103] I. Antoniadis, A possible new dimension at a few TeV, Phys. Lett. B **246**, 377 (1990).
[104] N. Arkani-Hamed and M. Schmaltz, Hierarchies without symmetries from extra dimensions, Phys. Rev. D **61**, 033005 (2000).
[105] D. E. Kaplan and T. M. P. Tait, New tools for fermion masses from extra dimensions, J. High Energy Phys. 11 (2001) 051.
[106] R. Kitano and T.-j. Li, Flavor hierarchy in SO(10) grand unified theories via five-dimensional wave function localization, Phys. Rev. D **67**, 116004 (2003).
[107] Y. Fujimoto, T. Nagasawa, K. Nishiwaki, and M. Sakamoto, Quark mass hierarchy and mixing via geometry of extra dimension with point interactions, Prog. Theor. Exp. Phys. **2013**, 023B07.
[108] C. Cai and H.-H. Zhang, Majorana neutrinos with point interactions, Phys. Rev. D **93**, 036003 (2016).
[109] H. Georgi, A. K. Grant, and G. Hailu, Chiral fermions, orbifolds, scalars and fat branes, Phys. Rev. D **63**, 064027 (2001).
[110] T. Appelquist, H.-C. Cheng, and B. A. Dobrescu, Bounds on universal extra dimensions, Phys. Rev. D **64**, 035002 (2001).
[111] D. Carmi, A. Falkowski, E. Kuflik, T. Volansky, and J. Zupan, Higgs after the discovery: A status report, J. High Energy Phys. 10 (2012) 196.
[112] Y. Fujimoto, T. Nagasawa, S. Ohya, and M. Sakamoto, Phase Structure of Gauge Theories on an Interval, Prog. Theor. Phys. **126** (2011) 841.
[113] ATLAS Collaboration, A search for resonant Higgs-pair production in the $b\bar{b}b\bar{b}$ final state in pp collisions at $\sqrt{s} = 8$ TeV, Report No. ATLAS-CONF-2014-005.
[114] R. S. Chivukula, D. A. Dicus, H.-J. He, and S. Nandi, Unitarity of the higher dimensional standard model, Phys. Lett. B **562**, 109 (2003).
[115] R. Mertig, M. Bohm, and A. Denner, FEYN CALC: Computer algebraic calculation of Feynman amplitudes, Comput. Phys. Commun. **64**, 345 (1991).
[116] T. Hahn and M. Perez-Victoria, Automatized one loop calculations in four-dimensions and D-dimensions, Comput. Phys. Commun. **118**, 153 (1999).
[117] J. Alwall, R. Frederix, S. Frixione, V. Hirschi, F. Maltoni, O. Mattelaer, H. S. Shao, T. Stelzer, P. Torrielli, and M. Zaro, The automated computation of tree-level and next-to-leading order differential cross sections, and their matching to parton shower simulations, J. High Energy Phys. 07 (2014) 079.
[118] A. Alloul, N. D. Christensen, C. Degrande, C. Duhr, and B. Fuks, FeynRules 2.0—A complete toolbox for tree-level phenomenology, Comput. Phys. Commun. **185**, 2250 (2014).
[119] G. Aad *et al.* (ATLAS Collaboration), Search for an additional, heavy Higgs boson in the $H \to ZZ$ decay channel at $\sqrt{s} = 8$ TeV in pp collision data with the ATLAS detector, Eur. Phys. J. C **76**, 45 (2016).
[120] V. Khachatryan *et al.* (CMS Collaboration), Search for a Higgs Boson in the Mass Range from 145 to 1000 GeV Decaying to a Pair of W or Z Bosons, J. High Energy Phys. 10 (2015) 144.
[121] G. Aad *et al.* (ATLAS Collaboration), Search for a high-mass Higgs boson decaying to a W boson pair in pp collisions at $\sqrt{s} = 8$ TeV with the ATLAS detector, J. High Energy Phys. 01 (2016) 032.
[122] G. Aad *et al.* (ATLAS Collaboration), Search for new resonances in $W\gamma$ and $Z\gamma$ final states in pp collisions at $\sqrt{s} = 8$ TeV with the ATLAS detector, Phys. Lett. B **738**, 428 (2014).
[123] CMS Collaboration, Search for Resonances Decaying to Dijet Final States at $\sqrt{s} = 8$ TeV with Scouting Data, Report No. CMS-PAS-EXO-14-005.
[124] G. Aad *et al.* (ATLAS Collaboration), Search for new phenomena in the dijet mass distribution using $p - p$ collision data at $\sqrt{s} = 8$ TeV with the ATLAS detector, Phys. Rev. D **91**, 052007 (2015).